

Visible light induced photo-oxidation of water. Formation of intermediary hydroxyl radicals through the photoexcited triplet state of perfluorophenazine

Takayuki Kitamura,^a Hiroyuki Fudemoto,^a Yuji Wada,^a Kei Murakoshi,^a Mitsuhiro Kusaba,^{b†} Nobuaki Nakashima,^{b*} Tetsuro Majima^c and Shozo Yanagida^{a*}

^a Material and Life Science, Graduate School of Engineering, Osaka University, Suita, Osaka 565, Japan

^b Institute of Laser Engineering, Osaka University, Suita, Osaka 565, Japan

^c The Institute of Scientific and Industrial Research, Osaka University, Ibaraki, Osaka 567, Japan

1,2,3,4,5,6,7,8-Octafluorophenazine (F-Phen) has an absorption spectrum in the longer wavelength extending to the visible-light region and has a more positive oxidation potential than for unfluorinated phenazine. F-Phen has been photolysed with water in acetonitrile under visible-light irradiation to produce stoichiometrically 1,3,4,5,6,7,8-heptafluoro-2-hydroxyphenazine (F-Phen-2-OH). Photolysis of F-Phen with water in the presence of benzene leads to the formation of phenol followed by the disappearance of F-Phen. EPR analysis and laser flash photolysis reveal that the photoexcited triplet state of F-Phen participates in water oxidation to hydroxyl radicals with concurrent conversion to F-Phen-2-OH. The mechanism is discussed with the results of semi-empirical molecular orbital calculations.

The photoassisted splitting of water molecules to hydrogen and oxygen has attracted much attention as a potential solar energy conversion and storage system.¹ In such systems, the development of efficient photosensitizers or photocatalysts to split water under visible-light irradiation is one of the important topics. We reported recently that perfluorinated poly- and oligo-*p*-phenylene)s (F-PPP-*n*, F-OPP-*n*; *n* denotes the number of phenyl rings in the chain) photosensitized catalytic oxidation of water to hydroxyl radicals under UV-light irradiation in the presence and absence of oxygen and that the resulting hydroxyl radicals were scavenged by benzene to give phenol.^{2–5} Spectroscopic analysis of transient spectra of perfluorinated *p*-terphenyl (F-OPP-3) as a model molecule of F-PPP-*n* and F-OPP-*n* revealed that the radical cation of F-OPP-3 formed from the photoexcited singlet state.⁵ Electrochemical analysis confirmed that F-OPP-3 had a more positive redox potential (high enough to oxidize water to hydroxyl radicals) than *p*-terphenyl (OPP-3).² In addition, semi-empirical molecular orbital calculations with MOPAC also suggested that perfluorination of aromatic molecules like OPP-3 should have resistance to oxidative degradation.²

In linear aromatic compounds *e.g.* a series of *p*-phenylenes, however, perfluorination induces a hypsochromic shift, and the bathochromic shift which is anticipated from an increase of chain length is found to be negligible.² This is interpreted as owing to an increase of the dihedral angles between the neighbouring phenyl rings because of the steric repulsion between large fluorine atoms at *ortho*-positions of the neighbouring phenyl rings. Such repulsion forbids their conjugation of the π electron system, resulting in the negligible bathochromic shift in absorption spectra even when the chain length is increased. On the other hand, we attempted to calculate the absorption spectra of perfluorinated condensed aromatic compounds by semi-empirical molecular orbital calculations with ZINDO.

The results indicated that they would have absorption spectra shifted to longer wavelength than the original aromatics. With these facts in mind, we aim to examine some perfluorinated condensed aromatics as photosensitizers for water oxidation under visible light irradiation.

In this paper, we deal with the photochemistry of 1,2,3,4,5,6,7,8-octafluorophenazine (perfluorophenazine, F-Phen) as an example of perfluorinated condensed aromatics that can absorb visible light, because its synthesis has been reported.⁶ The photophysical and electrochemical properties of F-Phen are characterized for the purpose of water oxidation under visible-light irradiation. We have now found that F-Phen induces photooxidation of water in its photoreaction.

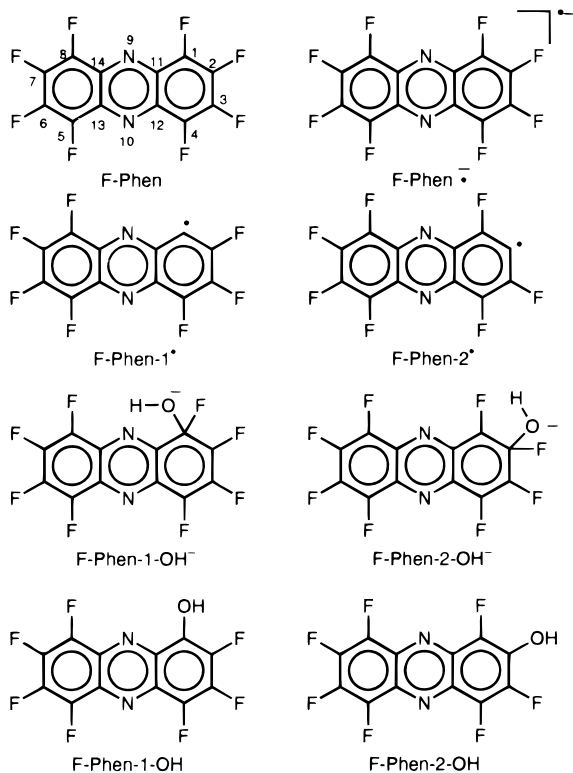
Experimental

Materials

For the synthesis of perfluorophenazine, commercially available 2,3,4,5,6-pentafluoroaniline (Aldrich, 99%) and lead tetraacetate (WAKO, Chemical reagent grade) were used without further purification, and benzene was used after distillation in the presence of calcium hydride (CaH₂: EP grade). For spectroscopic measurements, acetonitrile (AN: GR grade), cyclohexane (CH: Spectro grade) and 1-chlorobutane (BuCl: Spectro grade) were distilled in the presence of CaH₂, and 2-methyltetrahydrofuran (MTHF: GR grade) was distilled in the presence of sodium metal. Finally all the solvents were purified further by repeated bulb-to-bulb distillation in the presence of CaH₂ or Na. Tetrabutylammonium hexafluorophosphate (TBAPF₆: GR grade) was recrystallized three times from an EtOH–H₂O = 1:1 solution and dried at 45 °C *in vacuo* for 3 h before use for electrochemical measurements. AN used for electrochemical measurements was obtained by distillation three times in the presence of CaH₂. Iron(II) ammonium sulfate [Fe(NH₄)₂(SO₄)₂·6H₂O: EP Grade] and hydrogen peroxide (H₂O₂: EP grade) were used for Fenton reaction as received. 5,5-Dimethyl-1-pyrroline *N*-oxide (DMPO: Dojin, specially prepared reagent) as a spin trapping

† Present address: Laser Engineering Laboratory, Department of Electrical Engineering and Electronics, Faculty of Engineering, Osaka Sangyo University, Diato, Osaka 574, Japan.

* Present address: Department of Chemistry, Faculty of Science, Osaka City University, Sumiyoshi-ku, Osaka 558, Japan.



Scheme 1

reagent for EPR detection was used without further purification.

Instruments

Because perfluorinated compounds sublime so easily, melting points were obtained as extrapolated onsets by a differential scanning calorimetry method recorded on a Seiko Instruments, DSC 22C calorimeter (sample weight: 5 mg; temperature range: 30–300 °C; increase rate: 10 °C min⁻¹). ¹⁹F NMR spectra were recorded in CDCl₃, CD₃CN and CD₃COCD₃ at 254.05 MHz on a JEOL, JNM-EX 270 instrument. Chemical shift values were calibrated to trifluoroacetic acid at δ – 77.000 or 1,1,1-trichloro-2,2,2-trifluoroethane (CCl₃CF₃) at δ – 81.890 used as standards. UV–VIS absorption spectra, steady-state fluorescence spectra and lifetime of fluorescence were determined as reported previously.⁵ The fluorescence quantum yield was determined by using 9,10-diphenylanthracene in CH₂Cl₂ (0.90) as a standard. FTIR spectra were recorded on a Perkin-Elmer, System 200 FTIR spectrometer. GCMS analyses were conducted on a Shimadzu, GCMS-QP2000A instrument combined with a GC-14A [GC/column: Hi-Cap CBP-1 (equivalent to OV-1, 0.2 mm × 25 m); carrier gas: He; flow pressure: 1.0 kg cm⁻²; column temperature: 100–180 °C; injection temperature: 250 °C, MS/temperature: 250 °C; ionization: E_i (70 eV)]. EPR spectra were recorded on a JEOL, JES-RE2X spectrometer.

Preparation of 1,2,3,4,5,6,7,8-octafluorophenazine (F-Phen)

1,2,3,4,5,6,7,8-Octafluorophenazine (perfluorophenazine, F-Phen) was synthesized by Haszeldine's method⁶ as follows. In a three-necked flask with a condenser, lead tetraacetate (25.0 g, 55 mmol) was added to a benzene solution (0.15 dm³) of 2,3,4,5,6-pentafluoroaniline (5.0 g, 27 mmol), and the mixture was heated under reflux for 1 h. The resulting dark brown suspension was washed successively with 50% aqueous acetic acid, water, saturated aqueous sodium hydrogen carbonate, and saturated aqueous sodium chloride, and the resulting organic phase was dried with magnesium sulfate and

evaporated to dryness under reduced pressure, giving a black residue (4.71 g). The residue was chromatographed over silica gel. After orange perfluoroazobenzene was eluted by cyclohexane–benzene = 9:1, light orange F-Phen was eluted by benzene. Recrystallization from benzene gave light-orange coloured F-Phen (0.92 g, 20%), mp 234 °C (lit.,⁶ 239, and lit.,⁷ 234); $\delta_{\text{F}}(\text{CDCl}_3)$ – 150.36 (d, 2-F) and – 146.13 (d, 1-F); m/z (E_i) 324 (M⁺, 100%).

Electrochemical measurements

The redox potentials of F-Phen and Phen in AN solution were measured by cyclic voltammetry using an argon-purged AN solution containing F-Phen or Phen (2×10^{-3} mol dm⁻³) and TBAPF₆ (0.2 mol dm⁻³) as a supporting electrolyte. Redox potentials were standardized by Ag/0.01 mol dm⁻³ AgNO₃ as a reference electrode and platinum wires (ϕ = 0.3 mm) were used as working and counter electrodes.

Photoreactions of F-Phen with water

Photoreaction monitored by UV–VIS spectroscopy. In a quartz cuvette cell (optical pathlength: d = 10 mm), an AN solution (3×10^{-3} dm³) containing F-Phen (1×10^{-4} mol dm⁻³) and H₂O (0.06×10^{-3} dm³: 1.1 mol dm⁻³) was degassed by freeze–pump–thaw cycles and sealed, and the solution was then irradiated by a 300 W halogen–tungsten lamp through a saturated sodium nitrite filter (λ > 400 nm). The reaction was followed by UV–VIS spectrometer.

Photoreactions followed by products analysis. In a Pyrex tube (id = 8 mm), an AN (2×10^{-3} dm³) solution containing F-Phen (1×10^{-3} mol dm⁻³) and water (0.04×10^{-3} dm³: 1.1 mol dm⁻³) was irradiated after the system was purged with argon to eliminate dissolved air and oxygen. Photolysis, in the presence of benzene, was carried out in a Pyrex tube (id = 8 mm), on an AN (2×10^{-3} dm³) solution containing F-Phen (1×10^{-3} mol dm⁻³), water (0.04×10^{-3} dm³: 1.1 mol dm⁻³) and benzene (0.4×10^{-3} dm³: 4.5 mol dm⁻³) under an atmosphere of argon or oxygen gas.² The amount of F-Phen was determined by HPLC [column: Nacalai Tesque, COSMOSIL 5C18–water (4.6 mm × 250 mm); eluant: AN: water (w/w) = 50: 50; flow rate: 600×10^{-3} dm³ min⁻¹; UV detector: λ = 254 nm]. Phenol was analysed by GLC [column: PEG-20M (5%) (3 mm × 1 m); carrier gas: N₂; flow rate: 30×10^{-3} dm³ min⁻¹; column temperature: 160 °C; injection temperature: 190 °C; detector: FID], and hydrogen peroxide by colorimetry using a methanolic Ti(SO₄)₂ solution.²

Photoreaction monitored by ¹⁹F NMR spectroscopy. A CD₃CN solution (1×10^{-3} dm³) containing F-Phen (5.4×10^{-3} mol dm⁻³) and H₂O (0.05×10^{-3} dm³: 2.8 mol dm⁻³) was placed in an NMR tube with trifluoroacetic acid sealed in a glass capillary as an external standard and then purged with argon gas. The solution was irradiated for 9 h under the same conditions described in the above section. One couple of doublet signals of F-Phen faded out and then eight signals appeared by visible-light irradiation, assigned as/duo to the formation of 1,3,4,5,6,7,8-heptafluoro-2-hydroxyphenazine (F-Phen-2-OH) as described in the identification of the photoproduct as 1,3,4,5,6,7,8-heptafluoro-2-hydroxyphenazine (F-Phen-2-OH) and in the molecular orbital calculations sections. The signal observed at δ – 177.42 was ascribed to hydrogen fluoride (HF). ¹⁹F NMR before irradiation: $\delta_{\text{F}}(\text{aqueous CD}_3\text{CN})$ – 151.86 (d, 2-F) and – 148.69 (d, 1-F); ¹⁹F NMR after 9 h irradiation: $\delta_{\text{F}}(\text{aqueous CD}_3\text{CN})$ – 177.42 (s, br, HF), – 161.26 (d, 1-F), – 152.93 (d, 3-F), – 152.48 (dd, 6-F), – 151.91 (dd, 7-F), – 150.93 (dd, 8-F), – 150.44 (dd, 5-F), – 148.37 (dd, 4-F).

Fenton reaction.⁸ Into a mixture of the same quantity ($10 \times 10^{-3} \text{ dm}^3$) of an aqueous solution of $\text{Fe}(\text{NH}_4)_2(\text{SO}_4)_2$ (0.36 mol dm^{-3}) and an AN solution of F-Phen ($1 \times 10^{-3} \text{ mol dm}^{-3}$), an aqueous solution of 30% H_2O_2 ($10 \times 10^{-3} \text{ dm}^3$) was added dropwise under stirring at room temperature. The resulting red solution was condensed under reduced pressure and then the aqueous residue was extracted with diethyl ether. The extract was dried with sodium sulfide, condensed and analysed by GC-MS.

Identification of the photoproduct as 1,3,4,5,6,7,8-heptafluoro-2-hydroxyphenazine (F-Phen-2-OH). The reaction mixture was evaporated to dryness under reduced pressure and the residue was purified by using recycling gel permeation chromatography as described previously.⁵ The collected fraction was evaporated *in vacuo* and the orange-coloured photoproduct was analysed by IR, MS and ^{19}F NMR spectroscopy: mp 259°C (decomp.); MS: m/z (EI) 322 (M^+ , 100); IR: $\nu_{\text{max}}(\text{KBr})/\text{cm}^{-1}$ 3360 (br, O—H stretching), 1680, 1580, 1520, 1490 and 1360 (aromatic ring stretching), 1330 (O—H in-plane bending), 1080 and 1060 (C—F stretching). ^{19}F NMR analysis gave the following seven signals with the same integral value. From the ^{19}F - ^{19}F COSY spectrum the signals were assigned on the basis of the specific coupling between *ortho*- and *para*-fluorine atoms with $J = 15 \text{ Hz}$ at the benzenoid rings and the charge density at each fluorine atom determined by semi-empirical molecular orbital (MO) calculations using MOPAC (see the molecular orbital calculations section and Scheme 1) as follows; $\delta_{\text{F}}(\text{CD}_3\text{CN}) - 162.54$ (d, 1-F), -154.46 (d, 3-F), -153.92 (dd, 6-F), -153.41 (dd, 7-F), -152.25 (dd, 8-F), -151.94 (dd, 5-F), -149.92 (dd, 4-F).

Hudson *et al.* reported that F-Phen-2-OH should be produced by the nucleophilic substitution reaction of F-Phen

with hydroxide ion (OH^-) by assuming that the transient *p*-quinonoid structure of the OH^- adduct might be favourable for production of F-Phen-2-OH.⁹ However, the Hudson's product we prepared was assigned to 2,3,4,5,6,7,8-heptafluoro-1-hydroxyphenazine (F-Phen-1-OH) on the basis of the following analysis; mp 267°C (decomp.) (lit.⁹ $272-273$); m/z (EI) 322 (M^+ , 100); $\nu_{\text{max}}(\text{KBr})/\text{cm}^{-1}$ 3100 (br, O—H stretching), 1680, 1580, 1520, 1500 and 1360 (aromatic ring stretching), 1300 (O—H in-plane bending), 1090 and 1050 (C—F stretching); $\delta_{\text{F}}(\text{CD}_3\text{COCD}_3) - 155.59$ (d, 2-F), -155.37 (dd, 3-F), -153.88 (dd, 6-F), -153.82 (dd, 7-F), -153.55 (dd, 8-F), -152.53 (dd, 5-F), -145.83 (d, 4-F) (see Scheme 1). ^{19}F NMR analysis gave the seven signals with the same integral value, which were different from those of our product (F-Phen-2-OH).

The assignment was also supported by MO calculations using MOPAC (see the molecular orbital calculations section) as follows; (i) C(1) of F-Phen was more favourable for nucleophilic attack than C(2), because the partial charge of the former was more positive than the latter (ii) the heats of formation of the intermediary OH^- adduct at C(1) were smaller by 1.9 – $5.3 \text{ kcal mol}^{-1}$ than that of the OH^- adduct at C(2).

The difference in the wavenumber of the O—H bond bending between F-Phen-1-OH ($\nu_{\text{max}} = 1300 \text{ cm}^{-1}$) and F-Phen-2-OH ($\nu_{\text{max}} = 1330 \text{ cm}^{-1}$) was worth noting for validity of the assignment. This observation could be explained by the fact that the O—H bending vibration should be restricted by the intramolecular interaction of hydroxy group with the lone pair electron of the nitrogen atom in F-Phen-1-OH rather than in F-Phen-2-OH. In fact, the O—H bond faced toward the nitrogen atom in the energetically stable structure of F-Phen-1-OH optimized by the MO calculations [Fig. 1(a)].

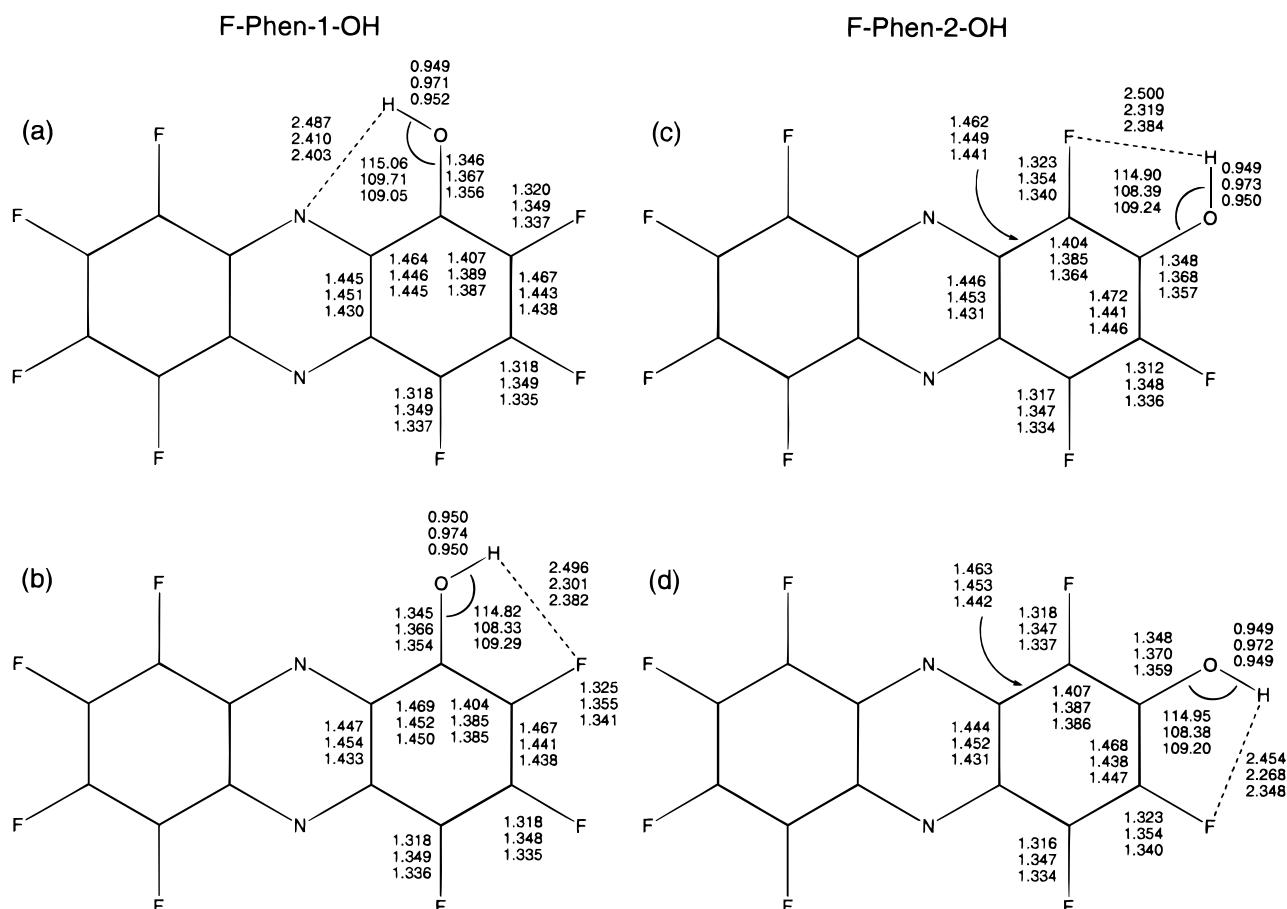


Fig. 1 Energetically optimized geometries of monohydroxylated F-Phen (F-Phen-1-OH and F-Phen-2-OH) by MOPAC with various Hamiltonians: upper MND0; middle AM1; lower PM3, bond lengths and atom distances in Å and bond angles in degrees.

Table 1 Heats of formation of F-Phen, products and intermediary species from F-Phen calculated by MOPAC^a

species	MNDO	AM1	AM1–MNDO	PM3	PM3–MNDO
F-Phen	–277.40242	–239.54184	–269.74069	–251.55998	–271.49621
F-Phen ^{•-}	–353.14860	–308.21576	–349.04179	– ^b	– ^b
F-Phen-1 [•]	–174.86385	–135.45257	–168.15920	–147.10089	–168.54403
F-Phen-2 [•]	–175.86014	–136.49589	–169.31097	–146.66409	–169.79025
F-Phen-1-OH ⁻	–405.22582	–362.74984	–395.63411	–380.12684	–399.00656
F-Phen-2-OH ⁻	–403.36323	–360.33016	–393.34903	–375.79105	–393.75391
F-Phen-1-OH(a)	–283.29969	–241.54721	–275.25095	–255.32942	–276.94425
F-Phen-1-OH(b)	–281.36712	–240.30860	–272.57516	–253.81621	–275.08952
F-Phen-2-OH(c)	–281.94545	–241.57796	–273.18574	–253.85426	–275.62634
F-Phen-2-OH(d)	–281.34804	–241.04784	–272.54397	–253.28083	–275.02574

^a Structural geometries were optimized energetically by using MNDO, AM1 and PM3 Hamiltonians, respectively. The 1SCF energy calculations were repeated by using MNDO Hamiltonian about the optimized structures obtained with AM1 and PM3 Hamiltonians. ^b Optimization of structure of F-Phen^{•-} failed in the SCF calculations.

Table 2 Partial charges of atoms of F-Phen calculated by MOPAC^a

position	MNDO	AM1	AM1–MNDO	PM3	PM3–MNDO
C(1),(4),(5),(8)	0.1717	0.0982	0.1773	0.0840	0.1763
C(2),(3),(6),(7)	0.1298	0.0575	0.1382	0.0475	0.1352
N(9),(10)	–0.1071	–0.0468	–0.1015	0.0490	–0.1092
C(11),(12),(13),(14)	0.0169	–0.0239	0.0189	–0.0566	0.0194
F(1),(4),(5),(8)	–0.1288	–0.0506	–0.1390	–0.0485	–0.1355
F(2),(3),(6),(7)	–0.1360	–0.0578	–0.1446	–0.0509	–0.1409

^a Structural geometries were optimized energetically by using MNDO, AM1 and PM3 Hamiltonians, respectively. The 1SCF energy calculations were repeated by using MNDO Hamiltonian about the optimized structures obtained with AM1 and PM3 Hamiltonians.

EPR analysis

An AN solution containing F-Phen (1×10^{-3} mol dm⁻³), water (1.1 mol dm⁻³), and DMPO (0.1 mol dm⁻³) was placed in an EPR tube ($d = 2.6$ mm) and degassed by freeze–pump–thaw cycles. The spectrum was recorded at room temperature during irradiation with a 500 W high-pressure mercury arc lamp through a 390 nm cut-off filter under the following conditions: magnetic field, 338 ± 7.5 mT; field modulation width, 0.01 mT; microwave power, 4 mW. Isotropic simulations of the EPR signals were performed on a JEOL, System ESPRIT-330 ver. 1.205 instrument.

Laser flash photolysis

An AN solution containing F-Phen was placed into a rectangular quartz cell ($d = 40 \times 10 \times 10$ mm) and then degassed by repeated freeze–pump–thaw cycles. The sample was irradiated by the fundamental of an XeF-excimer laser (Lambda Physik, EMG 201 MSC; peak power at $\lambda = 351$ nm,

pulse duration: 30 ns). Other instruments and conditions were the same as in the previous paper.⁵

γ -Radiolysis

Each solution in a Supersil cell ($d = 1.5$ mm) containing F-Phen (5×10^{-3} mol dm⁻³) in dry BuCl or MTHF was degassed by freeze–pump–thaw cycles and sealed *in vacuo*. γ -Radiolysis was conducted in the same way as in the previous paper.⁵

Molecular orbital calculations

Procedure of molecular orbital calculations. The geometric and electronic structures of F-Phen, products and intermediary species from F-Phen, *i.e.*, F-Phen, F-Phen^{•-}, two isomers of the F⁻-eliminated neutral radicals (F-Phen-1[•] and F-Phen-2[•]), two isomers of the intermediary OH⁻ adducts of F-Phen (F-Phen-1-OH⁻ and F-Phen-2-OH⁻) and two conformations of two isomers of monohydroxylated F-Phen (F-Phen-1-OH and F-Phen-2-OH) (Scheme 1), were obtained by semi-empirical molecular orbital (MO) calculations using MOPAC (ver. 6.10) in the CAChe Worksystem (ver. 3; CAChe Scientific, Inc.). Geometries were optimized energetically by using MNDO, AM1 and PM3 Hamiltonians, respectively. Then the 1SCF energy calculations were made again by using MNDO Hamiltonian about the optimized structures obtained with AM1 and PM3 Hamiltonians. The results of the calculations are summarized in Table 1–4 and Fig. 1. Optimization of the structure of F-Phen^{•-} by the PM3 Hamiltonian failed in the SCF calculations.

Heats of formation. Table 1 lists the heats of formation of all the species. Among the two F⁻-eliminated neutral radicals from F-Phen^{•-}, F-Phen-2[•] was more stable than F-Phen-1[•] by 1.0–1.2 kcal mol⁻¹. The heats of formation of F-Phen-1-OH⁻ were smaller by 1.9–5.3 kcal mol⁻¹ than that of F-Phen-2-OH⁻. Both F-Phen-1-OH and F-Phen-2-OH had two optimized conformations with local minima in energy, where all of the atoms were in the same plane and the directions of the O–H bonds were different to each other as shown in Fig. 1. The differences in the heats of formation between the respective conformations were only 1.3–2.7 kcal mol⁻¹. In F-Phen-

Table 3 Partial charges of atoms of F-Phen^{•-} calculated by MOPAC^a

position	MNDO	AM1	AM1–MNDO
C(1),(5)	0.0598	–0.0020	0.0662
C(2),(6)	0.1190	0.0438	0.1289
C(3),(7)	0.0213	–0.0308	0.0366
C(4),(8)	0.1403	0.0597	0.1407
N(9),(10)	–0.2275	–0.1730	–0.2245
C(11),(13)	0.0738	0.0283	0.0738
C(12),(14)	–0.0148	–0.0397	–0.0066
F(1),(5)	–0.1610	–0.0901	–0.1729
F(2),(6)	–0.1732	–0.1021	–0.1834
F(3),(7)	–0.1745	–0.1026	–0.1836
F(4),(8)	–0.1631	–0.0915	–0.1750

^a Structural geometries were optimized energetically by using MNDO and AM1 Hamiltonians, respectively. The 1SCF energy calculations were repeated by using the MNDO Hamiltonian about the optimized structures obtained with AM1 Hamiltonians.

Table 4 Partial charges of atoms of F-Phen-1-OH and F-Phen-2-OH calculated by MOPAC^a

position	F-Phen-1-OH									
	MNDO		AM1		AM1–MNDO		PM3		PM3–MNDO	
	(a)	(b)	(a)	(b)	(a)	(b)	(a)	(b)	(a)	(b)
C(1)	0.1341	0.1575	0.0838	0.1046	0.1180	0.1430	0.1325	0.1111	0.1453	0.1195
C(2)	0.1048	0.0303	0.0524	−0.0264	0.1187	0.0422	−0.0596	0.0168	0.0397	0.1138
C(3)	0.1545	0.1641	0.0759	0.0863	0.1611	0.1724	0.0809	0.0721	0.1683	0.1585
C(4)	0.1366	0.1349	0.0716	0.0695	0.1437	0.1420	0.0474	0.0483	0.1414	0.1428
C(5)	0.1759	0.1699	0.1016	0.0956	0.1814	0.1752	0.0819	0.0881	0.1745	0.1804
C(6)	0.1238	0.1289	0.0533	0.0585	0.1324	0.1378	0.0473	0.0421	0.1345	0.1294
C(7)	0.1335	0.1221	0.0614	0.0512	0.1418	0.1308	0.0400	0.0517	0.1278	0.1390
C(8)	0.1622	0.1761	0.0901	0.1028	0.1682	0.1818	0.0884	0.0740	0.1806	0.1669
N(9)	−0.1509	−0.0955	−0.0876	−0.0299	−0.1448	−0.0890	0.0642	0.0077	−0.0998	−0.1526
N(10)	−0.1086	−0.1168	−0.0459	−0.0549	−0.1023	−0.1115	0.0358	0.0509	−0.1189	−0.1097
C(11)	−0.0019	0.0238	−0.0426	−0.0114	0.0012	0.0257	−0.0591	−0.0844	0.0273	0.0002
C(12)	0.0315	0.0312	−0.0131	−0.0124	0.0336	0.0327	−0.0408	−0.0420	0.0326	0.0346
C(13)	0.0170	0.0218	−0.0236	−0.0186	0.0185	0.0241	−0.0495	−0.0574	0.0240	0.0195
C(14)	0.0202	0.0020	−0.0189	−0.0365	0.0225	0.0043	−0.0719	−0.0520	0.0062	0.0229
F(2)	−0.1403	−0.1603	−0.0580	−0.0815	−0.1470	−0.1686	−0.0660	−0.0548	−0.1650	−0.1452
F(3)	−0.1383	−0.1394	−0.0595	−0.0603	−0.1475	−0.1480	−0.0546	−0.0537	−0.1445	−0.1437
F(4)	−0.1347	−0.1349	−0.0558	−0.0559	−0.1447	−0.1450	−0.0525	−0.0523	−0.1413	−0.1411
F(5)	−0.1284	−0.1301	−0.0499	−0.0519	−0.1387	−0.1403	−0.0495	−0.0482	−0.1369	−0.1351
F(6)	−0.1370	−0.1379	−0.0583	−0.0592	−0.1455	−0.1464	−0.0524	−0.0514	−0.1428	−0.1418
F(7)	−0.1369	−0.1386	−0.0582	−0.0599	−0.1455	−0.1471	−0.0529	−0.0515	−0.1434	−0.1418
F(8)	−0.1354	−0.1310	−0.0568	−0.0517	−0.1454	−0.1411	−0.0503	−0.0530	−0.1377	−0.1417
O	−0.2125	−0.1989	−0.2173	−0.1983	−0.2010	−0.1859	−0.1727	−0.1893	−0.1810	−0.1934
H	0.2306	0.2209	0.2553	0.2402	0.2212	0.2110	0.2136	0.2273	0.2092	0.2186

position	F-Phen-2-OH									
	MNDO		AM1		AM1–MNDO		PM3		PM3–MNDO	
	(c)	(d)	(c)	(d)	(c)	(d)	(c)	(d)	(c)	(d)
C(1)	0.0773	0.1482	0.0193	0.0934	0.0869	0.1588	−0.0177	0.0548	0.0865	0.1562
C(2)	0.1149	0.0930	0.0609	0.0414	0.1005	0.0773	0.0964	0.0757	0.1023	0.0794
C(3)	0.1397	0.0847	0.0762	0.0160	0.1486	0.0945	0.0498	−0.0066	0.1447	0.0923
C(4)	0.1731	0.1922	0.1015	0.1184	0.1800	0.1991	0.0875	0.1036	0.1782	0.1966
C(5)	0.1770	0.1751	0.1024	0.1008	0.1829	0.1810	0.0888	0.0866	0.1815	0.1796
C(6)	0.1212	0.1224	0.0512	0.0524	0.1297	0.1310	0.0396	0.0410	0.1270	0.1283
C(7)	0.1294	0.1290	0.0583	0.0577	0.1385	0.1378	0.0475	0.0465	0.1351	0.1344
C(8)	0.1679	0.1687	0.0948	0.0958	0.1732	0.1743	0.0801	0.0815	0.1726	0.1736
N(9)	−0.1209	−0.1167	−0.0576	−0.0540	−0.1155	−0.1116	0.0309	0.0375	−0.1226	−0.1184
N(10)	−0.1036	−0.1035	−0.0439	−0.0444	−0.0985	−0.0988	0.0550	0.0539	−0.1057	−0.1059
C(11)	0.0466	0.0350	0.0002	−0.0102	0.0487	0.0366	−0.0255	−0.0372	0.0478	0.0362
C(12)	0.0022	−0.0036	−0.0359	−0.0400	0.0050	0.0000	−0.0730	−0.0773	0.0057	0.0004
C(13)	0.0028	0.0042	−0.0342	−0.0331	0.0050	0.0064	−0.0698	−0.0682	0.0063	0.0078
C(14)	0.0229	0.0244	−0.0187	−0.0179	0.0249	0.0258	−0.0487	−0.0491	0.0249	0.0261
F(1)	−0.1532	−0.1331	−0.0748	−0.0508	−0.1634	−0.1415	−0.0635	−0.0523	−0.1597	−0.1397
F(3)	−0.1369	−0.1571	−0.0549	−0.0786	−0.1442	−0.1659	−0.0529	−0.0640	−0.1424	−0.1621
F(4)	−0.1316	−0.1312	−0.0523	−0.0520	−0.1420	−0.1413	−0.0509	−0.0508	−0.1385	−0.1381
F(5)	−0.1305	−0.1308	−0.0520	−0.0524	−0.1407	−0.1411	−0.0499	−0.0503	−0.1372	−0.1375
F(6)	−0.1387	−0.1385	−0.0599	−0.0598	−0.1470	−0.1469	−0.0528	−0.0528	−0.1434	−0.1433
F(7)	−0.1382	−0.1379	−0.0595	−0.0592	−0.1467	−0.1464	−0.0527	−0.0525	−0.1430	−0.1428
F(8)	−0.1312	−0.1301	−0.0529	−0.0516	−0.1415	−0.1403	−0.0505	−0.0496	−0.1380	−0.1368
O	−0.2147	−0.2156	−0.2129	−0.2138	−0.1985	−0.1996	−0.1868	−0.1863	−0.1948	−0.1955
H	0.2245	0.2213	0.2449	0.2418	0.2143	0.2108	0.2190	0.2158	0.2127	0.2092

^a Structural geometries were optimized energetically by using MNDO, AM1 and PM3 Hamiltonians, respectively. The 1SCF energy calculations were repeated by using MNDO Hamiltonian about the optimized structures obtained with AM1 and PM3 Hamiltonians.

1-OH, the conformation (a) whose O–H bond faced the nitrogen atom was found to be more stable than another conformation (b). In F-Phen-2-OH, the conformation (c) was more stable than (d).

Comparison between F-Phen and F-Phen[−]. The optimized geometries of F-Phen had D_{2h} symmetry, but F-Phen[−] had only C_2 symmetry. The C–F bonds in the MNDO-optimized F-Phen[−] were slightly lengthened when compared with those of F-Phen [from 1.316 to 1.322 (α -positions) and from 1.318 to

1.321 Å (β -positions)], but in the AM1-optimized F-Phen and F-Phen[−], the C–F bonds at the α -positions were shortened drastically [from 1.474 to 1.348 (1- and 5-position) or 1.353 Å (4- and 8-position)] and those of the β -positions were lengthened (from 1.349 to 1.353 Å).

The charge distribution of F-Phen also had D_{2h} symmetry, and the partial charge on fluorine atoms was slightly more negative at F(2) than at F(1). The partial charge on carbon atoms was more positive at C(1) than at C(2) (Table 2) leading to favourable OH[−] attack at C(1). In F-Phen[−], the charge distribution had C_2 symmetry and the partial charges on all

fluorine atoms increased and the difference in charge distribution at α - and β -positions became more remarkable (Table 3). On the other hand, the average partial charge of C(2) and C(3) was less positive than that of C(1) and C(4). These calculations suggest that the C–F bond should be more weaker at the β -position than at the α -position in F-Phen $^{\cdot-}$.

Explanation of the signal of F-Phen-1-OH and F-Phen-2-OH in ^{19}F NMR. In order to assign the signals of the present photoproduct and the Hudson's product in ^{19}F NMR, the charge densities of fluorine atoms on F-Phen-1-OH [(a) and (b)] and F-Phen-2-OH [(c) and (d)] were obtained as listed in Table 4. F(8) in both conformers of the two isomers were more negatively charged than F(5), so that its ^{19}F NMR signal should appear at higher magnetic field. In F-Phen-1-OH, F(4) was more negatively charged than F(2) in the two conformers. The assignment in F-Phen-2-OH was made by using the conformation (c), where F(1) was more electronically shielded than F(3).

These MO calculations support that fact that the F^- elimination should occur on the 2-position of F-Phen $^{\cdot-}$, and F-Phen $^{\cdot-}$ and HO^\cdot should be converted selectively into F-Phen-2-OH. In contrast, the nucleophilic addition of OH^- to F-Phen should occur at C(1) rather than C(2), giving F-Phen-1-OH selectively.

Results and Discussion

Photophysical characteristics

Perfluorophenazine (F-Phen) was prepared in 20% yield by the method of oxidation coupling of 2,3,4,5,6-pentafluoroaniline using lead tetraacetate.⁶ F-Phen showed absorption bands at $\lambda_{\text{max}} = 256$ and 368 nm, which were assigned to π - π^* and n - π^* transitions, respectively. When compared with those of phenazine (Phen), they shifted to longer wavelength and the onset of the n - π^* band reached the visible-light region ($\lambda > 450$ nm) (Fig. 2) as anticipated from MO calculations (ZINDO). These results are rationalized as owing to conjugation of aromatic π electrons in F-Phen with unshared p-electron pairs of the fluorine atoms. Molar absorption coefficients of each band of F-Phen were found to be lower [$\lambda_{\text{max}}(\text{AN}) = 256$ and 368 nm ($\epsilon = 110\,000$ and $9\,000$ $\text{dm}^3 \text{mol}^{-1} \text{cm}^{-1}$)] than those of Phen [$\lambda_{\text{max}}(\text{AN}) = 248$ and 363 nm ($\epsilon = 140\,000$ and $15\,000$ $\text{dm}^3 \text{mol}^{-1} \text{cm}^{-1}$)].

It is well known that Phen has very weak fluorescence and strong phosphorescence, because the singlet excited state of Phen ($^1\text{Phen}^*$) undergoes fast intersystem crossing, giving its triplet excited state ($^3\text{Phen}^*$). F-Phen showed an emission at $\lambda_{\text{max}} = 475$ nm by excitation of both bands of π - π^* and n - π^*

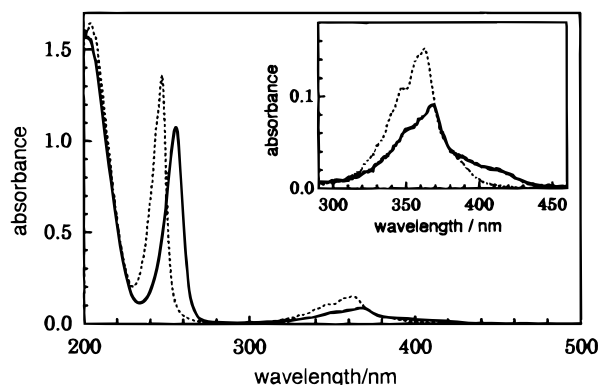


Fig. 2 Absorption spectra of F-Phen (—) and Phen (---) in an AN solution (1×10^{-5} mol dm^{-3}). Insert: Magnification of the absorption spectra.

in AN at room temperature (Fig. 3). The lifetime and quantum yield of the emission were determined to be 23 ns and 0.1, respectively, regardless of the excitation bands. The shape of the emission in AN was unchanged within the range of concentration of F-Phen from 1×10^{-6} to 5×10^{-3} mol dm^{-3} . The emission spectrum in cyclohexane (Fig. 3) shifted to shorter wavelength than in AN with vibrational structures due to the aromatic ring stretching (*ca.* 1500 cm^{-1}). These results suggest that the emission of F-Phen is ascribed to the n - π^* transition. F-Phen did not show phosphorescence in an ethanol glass matrix at 77 K, while Phen has a phosphorescence at around $\lambda = 640$ nm under the same conditions.¹⁰

Electrochemical properties

Redox potentials for reduction of F-Phen and Phen in AN were obtained by cyclic voltammetry. The reduction potential of Phen was -1.45 V *vs.* Ag/AgNO_3 , as observed by Sawyer *et al.* (-1.13 V *vs.* SCE^{11}). F-Phen was reduced reversibly to its radical anion by a cathodic sweep, and the redox potential was obtained as -0.89 V *vs.* Ag/AgNO_3 . This value is in contrast with the value of -1.45 V *vs.* Ag/AgNO_3 for Phen, indicating that perfluorination induces a positive shift in the redox potential by 0.6 V.

From the reduction potential and the difference between the energy of HOMO and LUMO, *i.e.*, the 0–0 band energy, 2.8 eV, determined from the excitation and emission spectra (Fig. 2), the redox potential of F-Phen/F-Phen $^{\cdot-}$ couple was calculated to be $+2.2$ V *vs.* SCE . It is difficult to measure redox potentials of the F-Phen $^{\cdot-}$ /F-Phen* and F-Phen*/F-Phen $^{\cdot+}$ couples. However, the redox potential of the F-Phen/F-Phen $^{\cdot+}$ couple could approximate to the energy level of not only the HOMO of F-Phen, but also either the lower SOMO of F-Phen* or the SOMO of F-Phen $^{\cdot+}$. Accordingly, the potential of the oxidizing species conceivable in the photo process of F-Phen would be much more positive than the redox potential of $\text{HO}^-/\text{HO}^\cdot$ in AN ($+0.8$ V *vs.* NHE in AN^{12}).

Photolysis of F-Phen with water

Taking into account that F-Phen absorbed visible light ($\lambda > 400$ nm) and that it had the redox potential for F-Phen/F-Phen $^{\cdot+}$ positive enough to oxidize water, we examined a visible-light photolysis of F-Phen in an aqueous AN solution under degassed conditions. Fig. 4 shows the change in the absorption spectrum of the photolysate. The absorption spectrum of F-Phen was changed with two isobestic points at $\lambda = 330$ and 420 nm. Under anhydrous conditions, such a

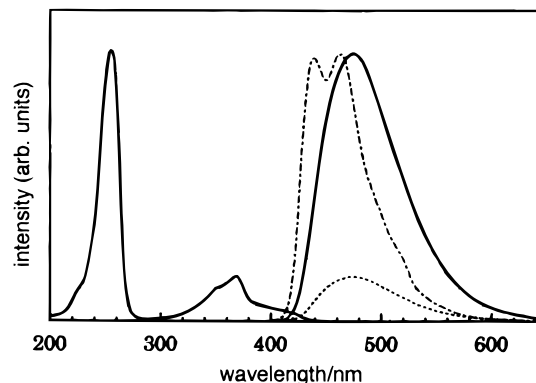


Fig. 3 Excitation and emission spectra of F-Phen: excitation spectrum monitored at $\lambda = 473$ nm (—); emission spectra irradiated at $\lambda = 256$ nm (—) and $\lambda = 368$ nm (---) in AN; emission spectrum irradiated at $\lambda = 258$ nm in CH (---); emission intensities were normalized.

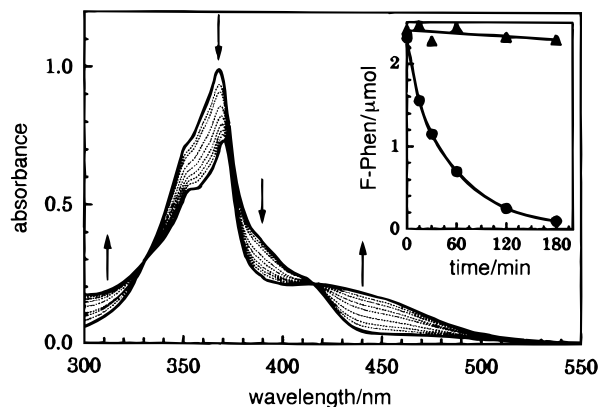


Fig. 4 Spectral change of F-Phen (1×10^{-4} mol dm $^{-3}$) in AN in the presence of water (2 vol.%: 1.1 mol dm $^{-3}$) under degassed conditions during the photo-irradiation with $\lambda > 400$ nm, the spectra were recorded after 0, 5, 20, 40, 60 and 80 min irradiation. Insert: Time conversion plots of photolysis of an AN solution (2×10^{-3} dm 3) of F-Phen (1×10^{-3} mol dm $^{-3}$) in the presence (●) and absence (▲) (2 vol.%: 1.1 mol dm $^{-3}$) of water with $\lambda > 400$ nm under degassed conditions.

change was found to be negligible (Fig. 4, insert). No change was observed when Phen was used instead of F-Phen.

These observations suggest that F-Phen should undergo stoichiometric transformation into another compound only in the presence of water by visible-light irradiation. During the photolysis monitored by ^{19}F NMR, the signals due to F-Phen disappeared with the appearance of eight new signals with same integral values. On examination of the photoproduct by ^{19}F NMR, IR spectroscopy and MS, we speculated the formation of hydroxylated F-Phen as a sole product. Further, the photoproduct was identified as 1,3,4,5,6,7,8-heptafluoro-2-hydroxyphenazine (F-Phen-2-OH) on the basis of the comparison with the previously reported hydroxylated F-Phen⁹ and the mechanistic analysis with the semi-empirical MO calculations (see Experimental). The characterization of the sole hydroxylated photoproduct suggests that hydroxyl radicals (HO^\bullet) should be formed through oxidation of H_2O in the photolysis with F-Phen under visible-light irradiation.

We also examined the visible-light photolysis of F-Phen with water by using benzene as a scavenger of HO^\bullet in an atmosphere of argon gas, as reported in the F-OPP-3-sensitized photohydroxylation of benzene to phenol (PhOH).² PhOH was formed and increased with reaction time (Fig. 5), and hydrogen peroxide (H_2O_2) derived from unremovable O_2

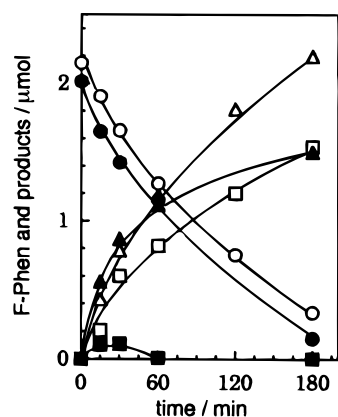


Fig. 5 Time conversion plots of photolysis of an AN solution of F-Phen (1×10^{-3} mol dm $^{-3}$) containing water (2 vol.%: 1.1 mol dm $^{-3}$) and benzene (20 vol.%: 4.5 mol dm $^{-3}$) under degassed (●, ▲, ■) and O_2 -saturated (○, △, □) conditions: (●, ○) F-Phen; (▲, △) PhOH; (■, □) H_2O_2 .

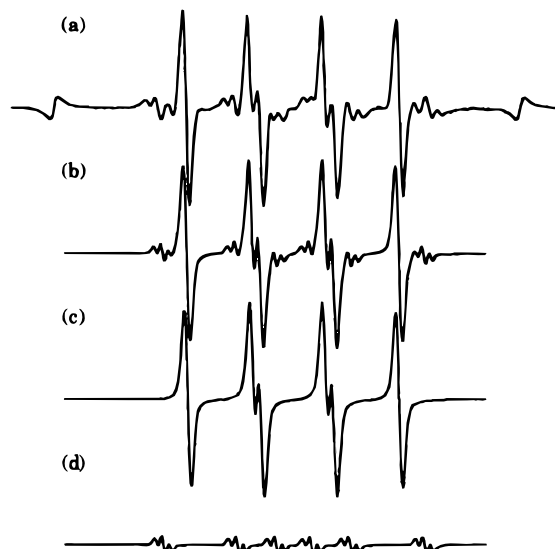


Fig. 6 Observed (a) and simulated [(b), (c), (d)] EPR spectra in an AN solution of F-Phen (1×10^{-3} mol dm $^{-3}$) containing water (2 vol.%) in the presence of DMPO (0.1 mol dm $^{-3}$) during irradiation ($\lambda > 390$ nm): (b) consisted of two signals (c) and (d) with an intensity ratio of 10:1; (c) $g = 2.006$, $a_{\text{N}} = 14.00$, $a_{\text{H}}^{\beta} = 12.45$; (d) $g = 2.006$, $a_{\text{N}} = 14.10$, $a_{\text{H}}^{\beta} = 21.50$, $a_{\text{H}}^{\alpha} = 1.30$.

was formed only in the early stages of photolysis. F-Phen disappeared gradually during the photolysis, and the quantities of the consumed F-Phen and of the formed PhOH were comparable. In order to suppress the possibility of reductive degradation of F-Phen, the photolysis was conducted in the presence of O_2 as an electron acceptor. The formation of PhOH and H_2O_2 was enhanced but the degradation of F-Phen was unavoidable (Fig. 5).

EPR detection of hydroxyl radicals (HO^\bullet)

In order to confirm the formation of HO^\bullet , F-Phen was irradiated in an aqueous AN solution containing DMPO as a spin-trapping reagent with visible light ($\lambda > 390$ nm) under degassed conditions, and EPR signals were measured as reported in the previous work.⁴ A main signal with six lines was obtained as shown in Fig. 6(a), and was assigned as the HO^\bullet adduct of DMPO by simulating its hyperfine splitting constants [hfsc, Fig. 6(c)].[†] In the absence of either F-Phen or water, no EPR signal was observed. These EPR analyses support the fact that F-Phen should play a crucial role in the formation of HO^\bullet due to the water oxidation in the present photoreaction system.

Determination of absorption spectra of intermediary radical ions from F-Phen by γ -radiolysis

An absorption spectrum of the radical anion of F-Phen ($\text{F-Phen}^{\bullet-}$) was obtained by γ -radiolysis in an MTHF glassy matrix cooled at 77 K and upon annealing to room temperature. In the MTHF matrix system at 77 K, the absorption spectrum gave some peaks in the region between $\lambda = 550$ and 700 nm, and these peaks decreased when the cold matrix was gradually warmed to room temperature (Fig. 7, insert). The difference spectrum obtained from each spectrum at 77 K and at room temperature showed four peaks at $\lambda = 460$, 570, 620 and 660 nm as $\text{F-Phen}^{\bullet-}$ (Fig. 7). The spectrum pattern was

[†] The small signal observed on EPR simulations as in Fig. 6(d) was not assigned, but judging from hfsc values, it was probably due to a DMPO adduct with an alkyl radical derived from DMPO itself.

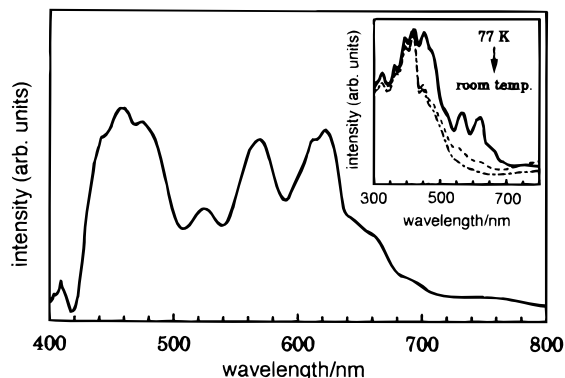


Fig. 7 Difference absorption spectra between 77 K and room temperature obtained after 1 h γ -radiolysis of F-Phen (2×10^{-3} mol dm^{-3}) in MTHF. Inset: Spectra obtained at 77 K and change on annealing to room temperature.

very similar to that of the radical anion of Phen,¹⁴ although it shifted to longer wavelength.

On the other hand, we failed to obtain the spectrum of the radical cation of F-Phen by γ -radiolysis in BuCl. The absorption spectrum observed at 77 K was identical with that of the radical cation of BuCl and warming of the system gave the spectrum of F-Phen only in the wavelength range 200–800 nm.

Observation of intermediary species from F-Phen by laser flash photolysis

We examined laser flash photolysis of F-Phen to ascertain short-lived intermediates photoformed from F-Phen. Fig. 8 shows a transient absorption spectrum of F-Phen in an AN solution obtained after pulse irradiation at $\lambda = 351$ nm under degassed conditions. This absorption with maxima at $\lambda = 430$ and 560 nm was assigned to the transition between excited triplet states of F-Phen ($^3\text{F-Phen}^*$), because it was similar to that of unfluorinated phenazine ($^3\text{Phen}^{*15}$) in shape and was quenched readily by addition of O_2 (Fig. 8, insert). The change of the absorbance of the transient spectrum monitored at $\lambda = 430$ and 560 nm followed a single exponential decay. The lifetime of $^3\text{F-Phen}^*$ was determined as 6.3 μs (Fig. 8, insert).

Introduction of water into the system induced a change of the decay of $^3\text{F-Phen}^*$. The transient absorption of $^3\text{F-Phen}^*$ was converted into a new one that showed absorption around $\lambda = 550$ –700 nm (Fig. 9). The resulting spectrum was similar to that of $\text{F-Phen}^{\cdot-}$ obtained in the γ -radiolysis in MTHF matrix (see Fig. 7).

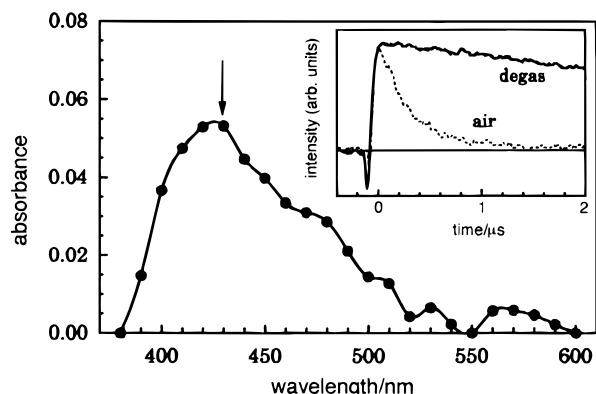


Fig. 8 Transient absorption spectrum obtained by laser flash photolysis of an AN solution of F-Phen (1×10^{-4} mol dm^{-3}) at 2 μs after the 30 ns pulse irradiation at $\lambda = 351$ nm. Inset: Decay of transient absorption monitored at $\lambda = 430$ nm under degassed (—) and aerated conditions (-----).

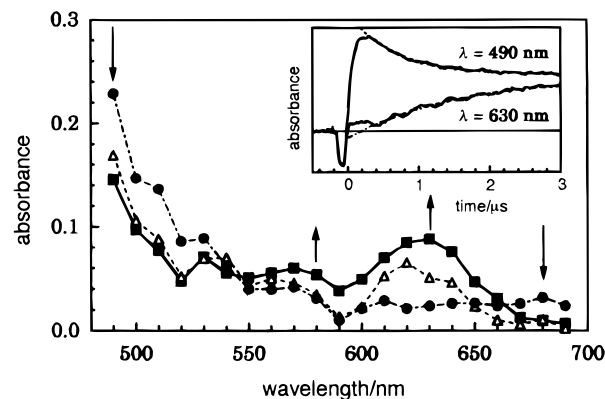


Fig. 9 Transient absorption spectra obtained by laser flash photolysis of an AN solution of F-Phen (1×10^{-3} mol dm^{-3}) in the presence of water (5 vol.%; 2.8 mol dm^{-3}) at various time delays after the 30 ns pulse irradiation at $\lambda = 351$ nm: (—●—) 0.5 μs , (----△----) 1 μs , (—■—) 2 μs . Inset: Change of transient absorption monitored at $\lambda = 490$ and 630 nm, and their fitting curves.

We monitored the decay of the absorbance of $^3\text{F-Phen}^*$ at $\lambda = 490$ nm and the build-up of the absorbance of $\text{F-Phen}^{\cdot-}$ at $\lambda = 630$ nm in an aqueous AN solution. Both of them followed almost first-order kinetics and gave the rate constants 1.5 and 0.7×10^6 s^{-1} , respectively (Fig. 9, insert). Both rate constants were in the same order, 10^6 s^{-1} , supporting the fact that $^3\text{F-Phen}^*$ should contribute to the formation of $\text{F-Phen}^{\cdot-}$ in the presence of water. In other words, $^3\text{F-Phen}^*$ should abstract one electron from H_2O to give HO^\cdot followed by the formation of $\text{F-Phen}^{\cdot-}$.

Mechanism

A mechanism of photolysis of water with F-Phen is depicted in Schemes 2 and 3. The photoexcited triplet state of F-Phen ($^3\text{F-Phen}^*$) is formed by intersystem crossing from the singlet excited state of F-Phen (1). $^3\text{F-Phen}^*$ leads to oxidation of water to hydroxyl radicals in the reductive quenching process (2). The formation of HO^\cdot was ascertained by both EPR analysis and the phenol production in the photolysis with benzene. On the other hand, the reductively quenched $^3\text{F-Phen}^*$ results in the production of $\text{F-Phen}^{\cdot-}$ through electron transfer from water.

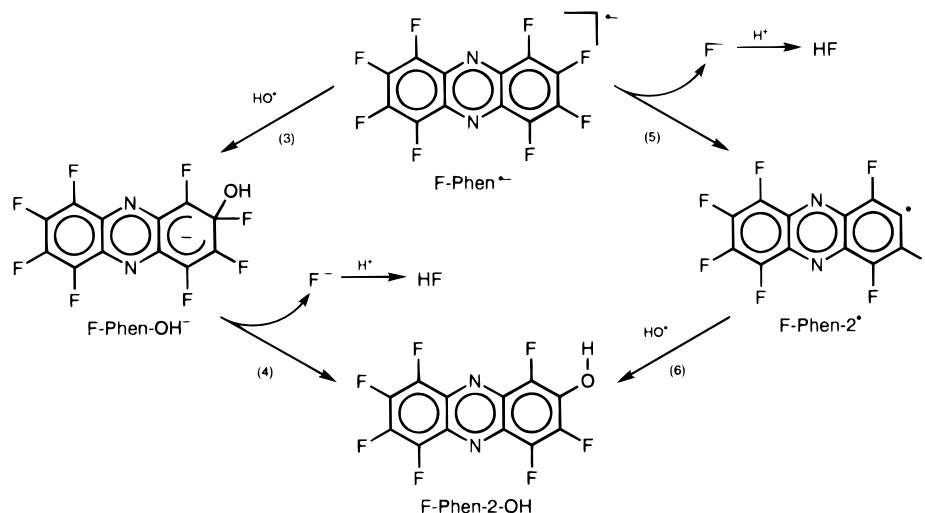
We propose here that both $\text{F-Phen}^{\cdot-}$ and HO^\cdot should participate in the formation of F-Phen-2-OH on the basis of the following facts; (i) the formation of F-Phen-2-OH was also detected in γ -radiolysis of F-Phen in aqueous MTHF where $\text{F-Phen}^{\cdot-}$ and HO^\cdot were formed, (ii) F-Phen-2-OH was not detected in Fenton's reaction where only HO^\cdot formed efficiently.

With regard to the bimolecular reaction between $\text{F-Phen}^{\cdot-}$ and HO^\cdot , two mechanisms are conceivable (Scheme 3), *i.e.*, the direct attack of HO^\cdot to $\text{F-Phen}^{\cdot-}$ followed by fluoride elimination [$\text{S}_{\text{RN}}2$ -like mechanism, (3) and (4)]¹⁶ and the coupling of HO^\cdot with $\text{F-Phen-2}^{\cdot-}$ formed by loss of fluoride from $\text{F-Phen-2}^{\cdot-}$ [$\text{S}_{\text{RN}}1$ -like mechanism, (5) and (6)].^{17,18}

On the MO calculations, the charge densities of carbon atoms of $\text{F-Phen}^{\cdot-}$ are less positive at β -positions than at α -positions (Table 3), causing hydroxyl radicals to attack preferably the carbon of β -positions. On the other hand, radical anions of polyfluoroaromatics fragment generally to form polyfluoroaromatic radicals and fluoride ion.¹⁷ Fluoride



Scheme 2



elimination from F-Phen^{•-} may occur at β -positions rather than α -positions, since the MO calculations indicate that the C—F bond at the β -position is more dissociative than the C—F bond at the α -position, and that the formation of F-Phen-2[•] from F-Phen^{•-} is energetically more favourable than that of F-Phen-1[•]. Thus, both of the S_{RN}2-like and S_{RN}1-like mechanisms are supported by the MO calculations.

In the present system, however, the stoichiometric formation of F-Phen-2-OH was confirmed spectroscopically, and we did not detect any hydrogenated or dimeric products which might form by reactions of F-Phen-2[•] with hydrogen donors like H₂O and other F-Phen-2[•] radicals. These facts imply that the S_{RN}2-like mechanism mainly contributes to the present system. In any event, the rapid coupling of HO[•] with F-Phen^{•-} and F-Phen-2[•] should occur possibly in a solvent cage, giving F-Phen-2-OH.

Conclusions

1,2,3,4,5,6,7,8-Octafluorophenazine (F-Phen) oxidizes water to yield HO[•] under visible-light ($\lambda > 400$ nm) irradiation. Long lived ³F-Phen* plays a decisive role as an oxidizing species in the oxidation of water. The photoexcited F-Phen is stoichiometrically converted into F-Phen-2-OH through the rapid coupling of HO[•] with F-Phen^{•-} and F-Phen-2[•] in a solvent cage. Success in the construction of electron mediating systems which suppress the concurrent reaction of F-Phen^{•-} could hopefully bring about water-splitting systems driven by visible light irradiation.

This work was supported by a Grant-in-Aid for Scientific Research (A) from the Ministry of Education, Science, Sports, and Culture of Japan (No. 06403023), partly defrayed by the Grant-in-Aid on Priority-Area-Research on 'Photoreaction Dynamics' from the Ministry of Education, Science, Sports, and Culture of Japan (No. 07228246), and the Institute of

Laser Technology under the commission of the Kansai Electric Power Company, Inc.

References

- (a) A. J. Bard and M. A. Fox, *Acc. Chem. Res.*, 1995, **28**, 141; (b) E. Amouyal, *Sol. Energy Mater. Sol. Cells*, 1995, **38**, 249 and references therein.
- K. Maruo, Y. Wada and S. Yanagida, *Bull. Chem. Soc. Jpn.*, 1992, **65**, 3439.
- K. Maruo, Y. Wada and S. Yanagida, *Chem. Lett.*, 1993, 565.
- T. Kitamura, K. Maruo, Y. Wada, K. Murakoshi, T. Akano and S. Yanagida, *J. Chem. Soc., Chem. Commun.*, 1995, 2189.
- T. Kitamura, Y. Wada, K. Murakoshi, M. Kusaba, N. Nakashima, A. Ishida, T. Majima, S. Takamuku, T. Akano and S. Yanagida, *J. Chem. Soc., Faraday Trans.*, 1996, **92**, 3491.
- J. M. Birchall, R. N. Haszeldine and J. E. G. Kemp, *J. Chem. Soc. C*, 1970, 449.
- A. G. Hudson, A. C. Pedler and J. C. Tatlow, *Tetrahedron Lett.*, 1968, **17**, 2143.
- (a) I. Yamazaki and L. H. Piette, *J. Biol. Chem.*, 1990, **265**, 13589; (b) *J. Am. Chem. Soc.*, 1991, **113**, 7588.
- A. G. Hudson, M. L. Jenkins, A. C. Pedler and J. C. Tatlow, *Tetrahedron*, 1970, **26**, 5781.
- (a) A. J. Kallir, G. W. Suter and U. P. Wild, *J. Lumin.*, 1984, **31** and **32**, 530; (b) *J. Phys. Chem.*, 1985, **89**, 1996.
- D. T. Sawyer and R. Y. Komai, *Anal. Chem.*, 1972, **44**, 715.
- L. Ebersson, *Acta Chem. Scand., Ser. B*, 1984, **38**, 439.
- G. R. Buettner, *Free Rad. Biol. Med.*, 1987, **3**, 259.
- T. Shida, *Electronic Absorption Spectra of Radical Ions*, Elsevier Science, New York, 1988, p. 180.
- Y. Hirata and I. Tanaka, *Chem. Phys. Lett.*, 1976, **43**, 568.
- (a) J. Marquet, Z. Jiang, I. Gallardo, A. Batlle and E. Cayón, *Tetrahedron Lett.*, 1993, **34**, 2801; (b) M. Mir, M. Espín, J. Marquet, I. Gallardo and C. Tomasi, *Tetrahedron Lett.*, 1993, **34**, 9055; (c) M. Niat, J. Marquet, I. Gallardo, M. Cervera and M. Mir, *Tetrahedron Lett.*, 1994, **35**, 9059.
- P. K. Freeman and R. Srinivasa, *J. Org. Chem.*, 1987, **52**, 252.
- L. C. T. Shoute and J. P. Mittal, *J. Phys. Chem.*, 1993, **97**, 379.

Paper 6/04920F; Received 12th July, 1996